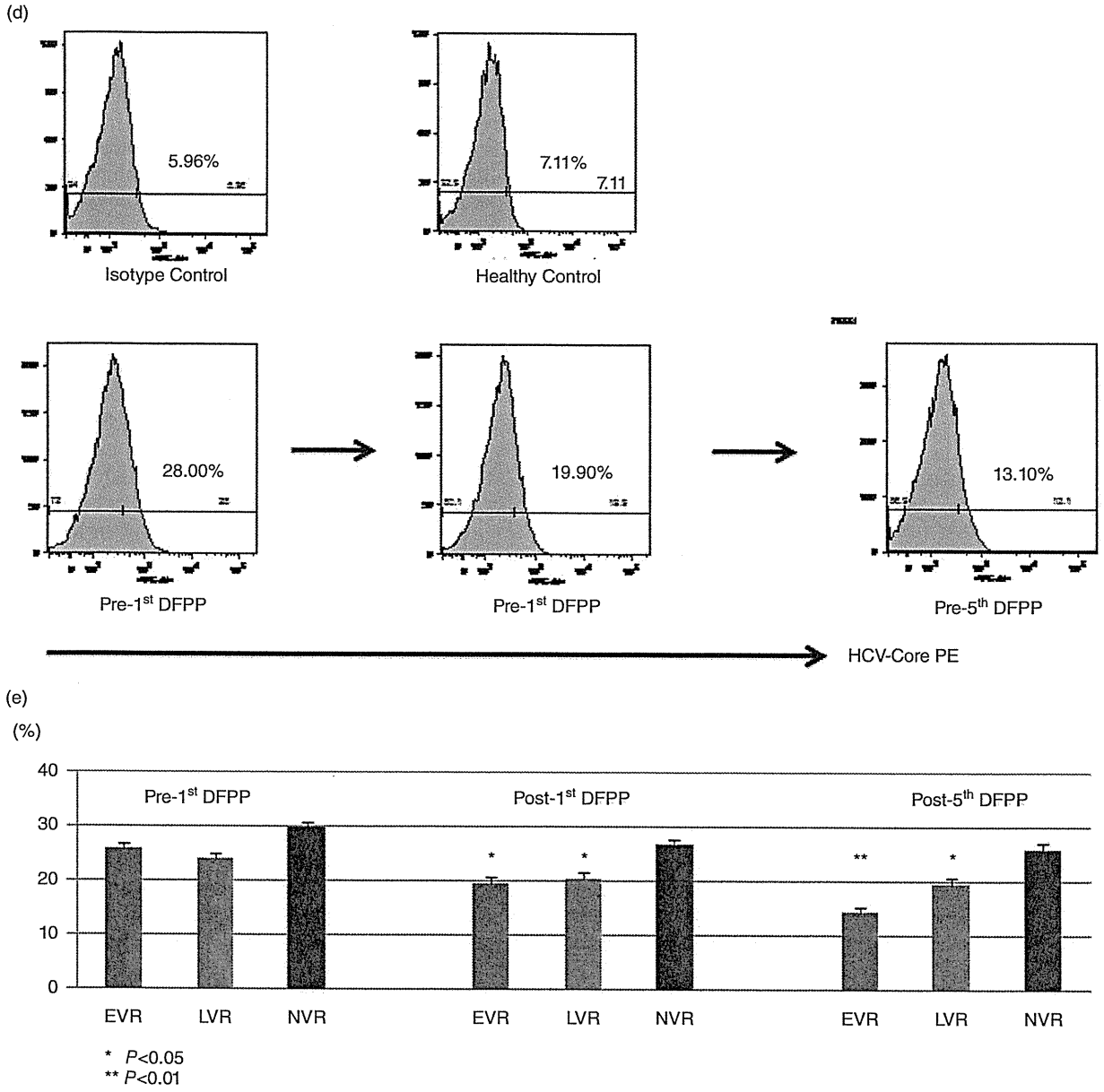


**Figure 4** *Continued.*

therapy and those who could achieve EVR by receiving Peg-IFN/RBV without the DFPP procedure (Fig. 4a–c and supplement Fig. S1). Moreover, the expression levels of STAT-1 and T-bet of patients treated with DFPP/Peg-IFN/RBV therapy were significantly higher than those treated with Peg-IFN/RBV therapy ($P < 0.01$) (Fig. 5). The amount of HCV-Core antigens was decreased during the first DFPP. Thus, in addition to HCV particles, free HCV-Core antigen might be able to be removed by DFPP. However, although the size of HCV-Core antigens is smaller than the target size of filtration, HCV-Core antigen binding with core-antibody and unknown proteins can be removed by DFPP. Then, we analyzed the surface binding of HCV-Core protein on $CD3^+$ T cells, which might affect STAT-1 signaling. We found a rapid reduction of HCV-Core protein on $CD3^+$ T cells in EVR patients in comparison to those of LVR and NVR ($P < 0.05$) (Fig. 4d,e).

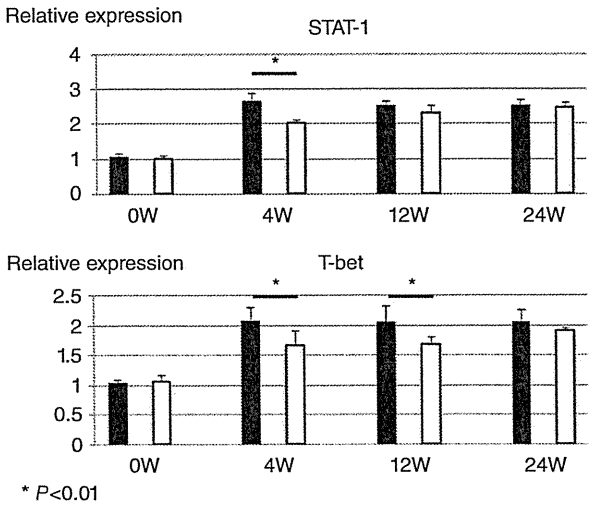


**Figure 5** Comparison of STAT-1 and T-bet expression between double filtration plasmapheresis combined with Peg-interferon and RBV (DFPP/Peg-IFN/RBV) and Peg-IFN/RBV therapy. The expression levels of STAT-1 and T-bet mRNA in CD4+ cells of early virological response (EVR) patients during IFN-based therapy (DFPP/Peg-IFN/RBV [$n = 5$] and Peg-IFN/RBV [$n = 5$]) were analyzed by realtime polymerase chain reaction (PCR). The relative expression levels are shown in bar graphs. The statistical analysis was carried out by independent student *t*-test.

## DISCUSSION

DOUBLE FILTRATION PLASMAPHERESIS has been applied for several kinds of auto-immune disease to reduce immunoglobulin-complex.[7,10,37] Recently, the efficacy of DFPP for the treatment of HCV was recognized in Japan and used especially in difficult-to-treat patients.[2,3] We selected 12 difficult-to-treat CHC-patients who had high HCV-RNA titers and genotype 1b HCV. DFPP therapy could not reduce the HCV-RNA in two patients who were previously null-responders with Peg-IFN/RBV therapy. Thus, the direct effect of DFPP for reducing the HCV particles is limited in null-responder patients. Previously, it has been reported that DFPP itself could affect immune cells by changing the lymphocyte subsets and stimulating the immune cells in peripheral blood.[5,10] Our data also indicated that the distributions of activated $CD3^+CD4^+$ and $CD3^+CD8^+$ T cells were changed after the 1st DFPP. Moreover, the $CD3^-CD16^-CD56^{high}$ NK cells that could vigorously produce various cytokines were increased in the peripheral blood of EVR patients after the DFPP procedure. These data indicated that DFPP could affect the distribution of lymphocyte subsets as previously reported. Moreover, the change of the distribution might differ among EVR, LVR and NVR at least in certain subsets of lymphocytes. The change of the lymphocyte distribution might contribute to the better response of DFPP/Peg-IFN/RBV therapy in comparison to the conventional Peg-IFN/RBV therapy.

Previously, we reported the direct effect of lymphotropic HCV in contributing to the Th1 immune suppression.[26,27] Most recently, we found that not only infection with HCV but also adding HCV particles could suppress the Th1 responsiveness by using human primary T lymphocyte.[25] In addition, another group reported that the binding of HCV-core proteins on T lymphocytes could suppress the STAT-1 signaling that might contribute to Th1 hypo-responsiveness. Therefore, we analyzed the amounts of HCV-Core antigens not only in the peripheral blood but also on the surfaces of T lymphocytes. The amounts of HCV-Core antigen in the peripheral blood of EVR patients were decreased more remarkably than those of LVR and NVR patients after the 1st DFPP. The remarkable reduction of HCV-Core antigen in EVR patients could be explained by the different levels of HCV-Core proteins released from hepatocytes according to the responsiveness to therapy. Another possible explanation might be the different amounts of free HCV-Core proteins that could not be trapped by the second filter since the target size of the second filter was larger than the HCV-Core proteins. Therefore, the existence of Immunoglobulin or unknown proteins binding with HCV-Core proteins that could be trapped by the second filter might be suggested in EVR patients. Moreover, the amounts of HCV-Core antigens on T lymphocytes were decreased more significantly in EVR patients than in LVR and NVR patients. The reduction of HCV-Core antigen and the mechanical stress of DFPP might contribute to the dissociation of HCV-Core antigen from T lymphocytes. In addition to T cells, NK cells might be affected by HCV-Core antigen. However, we could not analyze the dynamics in HCV core bound to NK cells due to the limitation of blood sampling.

We analyzed the amount of IFN-γ and IL10 not only in the plasma but also in the serum-free culture media with PBMCs after a 24-h incubation, since the amounts of IFN-γ and IL10 in the plasma of some patients were lower than the detection limits of ELISA. T cell receptor (TCR) stimulation with CD3 antibody could be used instead of non-stimulation. However, we thought the natural release of cytokines from PBMC with non-stimulation might be able to detect the effect of DFPP. The amounts of IFN-γ and IL10 produced from the PBMCs were changed after DFPP and differed among EVR, LVR and NVR. The ability of cytokine production from

PBMCs should be changed directly since the amount of cytokines in the plasma was not affected after DFPP in several patients that could be detected by ELISA (data not shown). The amounts of IFN-γ produced from PBMCs were gradually increased during DFPP/Peg-IFN/RBV therapy in EVR patients. On the other hand, the amounts of IL10 produced from PBMCs were gradually decreased during DFPP/Peg-IFN/RBV therapy in EVR patients.

In conclusion, the favorable effect of DFPP for HCV treatment might be due to not only the reduction of HCV but also the effect of immune reaction. DFPP itself could change the distribution of lymphocyte subsets, especially $CD3^{-}CD16^{-}CD56$high NK cells, in EVR patients and enhance the reduction of HCV-Core antigen binding on $CD3^{+}$ T cells. Accordingly, in this study, we could demonstrate this novel mechanism of DFPP for HCV treatment.

## ACKNOWLEDGEMENTS

WE ARE GRATEFUL to Koichi Kikuchi who belongs to the School of Medicine, Tohoku University for technical assistance. This work was supported in part by a Grant-in Aid from the Ministry of Education, Culture, Sport, Science, and Technology of Japan (Y.K. #23790761), and grants from Ministry of Health, Labor, and Welfare of Japan.

## REFERENCES

1 Poynard T, Yuen MF, Ratziu V, Lai CL. Viral hepatitis C. *Lancet* 2003; **362**: 2095–100.
2 Kaneko S, Sata M, Ide T *et al.* Efficacy and safety of double filtration plasmapheresis in combination with interferon therapy for chronic hepatitis C. *Hepatol Res* 2010; **40**: 1072–81.
3 Fujiwara K, Kaneko S, Kakumu S *et al.* Double filtration plasmapheresis and interferon combination therapy for chronic hepatitis C patients with genotype 1 and high viral load. *Hepatol Res* 2007; **37**: 701–10.
4 Yamashita T, Arai K, Sakai A *et al.* Virological effects and safety of combined double filtration plasmapheresis (DFPP) and interferon therapy in patients with chronic hepatitis C: a preliminary study. *Hepatol Res* 2006; **36**: 167–75.
5 Yeh JH, Chien PJ, Hsueh YM, Shih CM, Chiu HC. Changes in the lymphocyte subset after double-filtration plasmapheresis. *Am J Clin Pathol* 2007; **128**: 940–4.
6 Yeh JH, Chen WH, Chiu HC, Bai CH. Hemolysis in double-filtration plasmapheresis. *Am J Clin Pathol* 2007; **127**: 76–80.
7 Yamaji K, Tsuda H, Hashimoto H. A case report of the efficacy of apheresis for refractory autoimmune thrombocytopenia in a patient with systemic lupus erythematosus associated hemolytic anemia. *Ther Apher Dial* 2004; **8**: 227–31.
8 Ishizawa Y, Totsuka E, Umehara M, Nishimura A, Ono H, Sasaki M. Efficacy of double-filtration plasmapheretic cross-circulation with a high-permeability membrane using canine harvested liver in porcine fulminant hepatic failure model. *Transplant Proc* 2004; **36**: 2344–8.
9 Yamada H, Nagaoka I, Takamori K, Ogawa H. Double filtration plasmapheresis enhances neutrophil chemotactic responses in hyperimmunoglobulin E syndrome. *Artif Organs* 1995; **19**: 98–102.
10 Hatano Y, Katagiri K, Arakawa S, Umeki T, Takayasu S, Fujiwara S. Successful treatment by double-filtration plasmapheresis of a patient with bullous pemphigoid: effects *in vivo* on transcripts of several genes for chemokines and cytokines in peripheral blood mononuclear cells. *Br J Dermatol* 2003; **148**: 573–9.
11 Munemoto M, Otaki Y, Kasama S *et al.* Therapeutic efficacy of double filtration plasmapheresis in patients with anti-aquaporin-4 antibody-positive multiple sclerosis. *J Clin Neurosci* 2011; **18**: 478–80.
12 Ramunni A, De Robertis F, Brescia P *et al.* A case report of double filtration plasmapheresis in an acute episode of multiple sclerosis. *Ther Apher Dial* 2008; **12**: 250–4.
13 Liumbruno GM, Centoni PE, Niccoli G *et al.* A case report of long-term remission of ulcerative colitis after lymphocytoplasmapheresis. *Ther Apher Dial* 2007; **11**: 65–9.
14 Bosch T. Therapeutic apheresis – state of the art in the year 2005. *Ther Apher Dial* 2005; **9**: 459–68.
15 Nakamura T, Suzuki Y, Koide H. Granulocyte and monocyte adsorption apheresis in a patient with antiglomerular basement membrane glomerulonephritis and active ulcerative colitis. *Am J Med Sci* 2003; **325**: 296–8.
16 Tani T, Hanasawa K, Endo Y, Abe H, Numa K, Kodama M. Theoretical background of effect mechanism by extracorporeal immunomodulation. *Ther Apher* 1997; **1**: 219–23.
17 Koziel MJ. The role of immune responses in the pathogenesis of hepatitis C virus infection. *J Viral Hepat* 1997; 4 (Suppl 2): 31–41.
18 Rice CM, Walker CM. Hepatitis C virus-specific T lymphocyte responses. *Curr Opin Immunol* 1995; **7**: 532–8.
19 Chang KM, Rehermann B, Chisari FV. Immunopathology of hepatitis C. *Springer Semin Immunopathol* 1997; **19**: 57–68.
20 Blackburn SD, Wherry EJ. IL-10, T cell exhaustion and viral persistence. *Trends Microbiol* 2007; **15**: 143–6.
21 Bolacchi F, Sinistro A, Ciaprini C *et al.* Increased hepatitis C virus (HCV)-specific CD4+CD25+ regulatory T lymphocytes and reduced HCV-specific CD4+ T cell response in HCV-infected patients with normal versus abnormal alanine aminotransferase levels. *Clin Exp Immunol* 2006; **144**: 188–96.

22 Ulsenheimer A, Gerlach JT, Gruener NH *et al.* Detection of functionally altered hepatitis C virus-specific CD4 T cells in acute and chronic hepatitis C. *Hepatology* 2003; **37**: 1189–98.
23 Marshall NA, Vickers MA, Barker RN. Regulatory T cells secreting IL-10 dominate the immune response to EBV latent membrane protein 1. *J Immunol* 2003; **170**: 6183–9.
24 Cramp ME, Rossol S, Chokshi S, Carucci P, Williams R, Naoumov NV. Hepatitis C virus-specific T-cell reactivity during interferon and ribavirin treatment in chronic hepatitis C. *Gastroenterology* 2000; **118**: 346–55.
25 Kondo Y, Ueno Y, Kakazu E *et al.* Lymphotropic HCV strain can infect human primary naive CD4(+) cells and affect their proliferation and IFN-gamma secretion activity. *J Gastroenterol* 2011; **46**: 232–41.
26 Kondo Y, Machida K, Liu HM *et al.* Hepatitis C virus infection of T cells inhibits proliferation and enhances fas-mediated apoptosis by down-regulating the expression of CD44 splicing variant 6. *J Infect Dis* 2009; **199**: 726–36.
27 Kondo Y, Sung VM, Machida K, Liu M, Lai MM. Hepatitis C virus infects T cells and affects interferon-gamma signaling in T cell lines. *Virology* 2007; **361**: 161–73.
28 Yao ZQ, Prayther D, Trabue C, Dong ZP, Moorman J. Differential regulation of SOCS-1 signalling in B and T lymphocytes by hepatitis C virus core protein. *Immunology* 2008; **125**: 197–207.
29 Tacke RS, Tosello-Trampont A, Nguyen V, Mullins DW, Hahn YS. Extracellular hepatitis C virus core protein activates STAT3 in human monocyte/macrophage/dendritic cells via an IL-6 autocrine pathway. *J Biol Chem* 2011; **286**: 10 847–55.
30 Zhang Y, Ma CJ, Ni L *et al.* Cross-talk between programmed death-1 and suppressor of cytokine signaling-1 in inhibition of IL-12 production by monocytes/macrophages in hepatitis C virus infection. *J Immunol* 2011; **186**: 3093–103.
31 Akuta N, Suzuki F, Hirakawa M *et al.* Amino acid substitution in hepatitis C virus core region and genetic variation near the interleukin 28B gene predict viral response to telaprevir with peginterferon and ribavirin. *Hepatology* 2010; **52**: 421–9.
32 Thomas DL, Thio CL, Martin MP *et al.* Genetic variation in IL28B and spontaneous clearance of hepatitis C virus. *Nature* 2009; **461**: 798–801.
33 Tanaka Y, Nishida N, Sugiyama M *et al.* Genome-wide association of IL28B with response to pegylated interferon-alpha and ribavirin therapy for chronic hepatitis C. *Nat Genet* 2009; **41**: 1105–9.
34 Suppiah V, Moldovan M, Ahlenstiel G *et al.* IL28B is associated with response to chronic hepatitis C interferon-alpha and ribavirin therapy. *Nat Genet* 2009; **41**: 1100–4.
35 Ge D, Fellay J, Thompson AJ *et al.* Genetic variation in IL28B predicts hepatitis C treatment-induced viral clearance. *Nature* 2009; **461**: 399–401.
36 Kakazu E, Ueno Y, Kondo Y *et al.* Branched chain amino acids enhance the maturation and function of myeloid dendritic cells *ex vivo* in patients with advanced cirrhosis. *Hepatology* 2009; **50**: 1936–45.
37 Kobayashi T, Ando Y, Umino T *et al.* Complete remission of minimal-change nephrotic syndrome induced by apheresis monotherapy. *Clin Nephrol* 2006; **65**: 423–6.

## SUPPORTING INFORMATION

ADDITIONAL SUPPORTING INFORMATION may be found in the online version of this article:

**Figure S1** Comparison of the amounts of HCV-core antigen between DFPP/Peg-IFN/RBV and Peg-IFN/RBV therapy. A comparison of the amounts of HCV-core antigen between DFPP/Peg-IFN/RBV and Peg-IFN/RBV treated patients during therapy are shown. The case matched controls of the CHC patients who could achieve EVR with the same viral dynamics were selected ($n = 5$). The statistical analysis of these data was carried out by independent student t test.

Please note: Wiley-Blackwell are not responsible for the content or functionality of any supporting materials supplied by the authors. Any queries (other than missing material) should be directed to the corresponding author for the article.

J Gastroenterol (2011) 46:232–241
DOI 10.1007/s00535-010-0297-2

ORIGINAL ARTICLE—LIVER, PANCREAS, AND BILIARY TRACT

# Lymphotropic HCV strain can infect human primary naïve $CD4^+$ cells and affect their proliferation and IFN-$\gamma$ secretion activity

**Yasuteru Kondo · Yoshiyuki Ueno · Eiji Kakazu · Koju Kobayashi · Masaaki Shiina · Keiichi Tamai · Keigo Machida · Jun Inoue · Yuta Wakui · Koji Fukushima · Noriyuki Obara · Osamu Kimura · Tooru Shimosegawa**

Received: 9 May 2010 / Accepted: 11 July 2010 / Published online: 17 August 2010


## Abstract

*Background* Lymphotropic hepatitis C virus (HCV) infection of B and T cells might play an important role in the pathogenesis of hepatitis C. Recently, we showed that a lymphotropic HCV (SB strain) could infect established T-cell lines and B-cell lines. However, whether HCV replication interferes with cell proliferation and function in primary T lymphocytes is still unclear.

*Aim* The aim of this study was to analyze whether HCV replication in primary T lymphocytes affected their development, proliferation, and Th1 commitment.

*Methods* SB strain cell culture supernatant ($2 \times 10^4$ copies/ml HCV) was used to infect several kinds of primary lymphocyte subsets. Mock, UV-irradiated SB-HCV, JFH-1 strain, and JFH-1 NS5B mutant, which could not replicate in T cells, were included as negative controls. Carboxyfluorescein succinimidyl ester (CFSE) and CD45RA double staining was used to evaluate the proliferative activity of $CD4^+CD45RA^+CD45RO^-$ naïve $CD4^+$ cells. Interferon (IFN)-$\gamma$ and interleukin (IL)-10 secretion assays magnetic cell sorting (MACS) were carried out.

*Results* Negative strand HCV RNA was detected in $CD4^+$, $CD14^+$, and $CD19^+$ cells. Among $CD4^+$ cells, $CD4^+CD45RA^+RO^-$ cells (naïve $CD4^+$ cells) were most susceptible to replication of the SB strain. The levels of CFSE and CD45RA expression gradually declined during cell division in uninfected cells, while HCV-infected naïve $CD4^+$ cells expressed higher levels of CFSE and CD45RA than Mock or UV-SB infected naïve $CD4^+$ cells. Moreover, the production of IFN-$\gamma$ was significantly suppressed in SB-infected naïve $CD4^+$ cells.

*Conclusions* Lymphotropic HCV replication suppressed proliferation and development, including that towards Th1 commitment, in human primary naïve $CD4^+$ cells.

**Keywords** HCV · Lymphotropic · Naïve $CD4^+$ cell · Th1

**Electronic supplementary material** The online version of this article (doi:10.1007/s00535-010-0297-2) contains supplementary material, which is available to authorized users.

Y. Kondo · Y. Ueno (✉) · E. Kakazu · M. Shiina · K. Tamai · J. Inoue · Y. Wakui · K. Fukushima · N. Obara · O. Kimura · T. Shimosegawa
Division of Gastroenterology,
Tohoku University Graduate School of Medicine,
1-1 Seiryo, Aobaku, Sendai 980-8574, Japan
e-mail: yueno@med.tohoku.ac.jp

K. Machida
Department of Molecular Microbiology and Immunology,
University of Southern California Keck School of Medicine,
2011 Zonal Avenue, Los Angeles, CA 90033, USA

K. Kobayashi
School of Health Science, Tohoku University, 1-1 Seiryo,
Aobaku, Sendai 980-8574, Japan

## Introduction

Hepatitis C virus (HCV) infects about 170 million people worldwide and is a major cause of chronic hepatitis, liver cirrhosis, and hepatocellular carcinoma (HCC) [1]. Cellular and humoral immune responses to HCV play an important role in the pathogenesis of chronic hepatitis, liver cirrhosis, HCC, and B-lymphocyte proliferative disorders, including mixed cryoglobulinemia, a disorder characterized by the oligoclonal proliferation of B cells [2, 3].

Several mechanisms have been proposed for the failure of the cellular immune response, including anergy, cytotoxic T-lymphocyte (CTL) exhaustion, suppression via

regulatory $CD4^+$–$CD25^+$ T cells interleukin-10 (IL-10)-secreting regulatory $CD8^+$-T cells, and direct binding of HCV core antigen [4–7]. However, the influence of HCV replication in lymphoid cells on their functions is not fully understood. HCV replicates primarily in the liver, but HCV-RNA has been detected in other lymphoid cells, including B- and T-lymphocytes, monocytes, and dendritic cells [8–11]. Sung et al. [12] have previously reported a B-cell line (SB cells) that produces HCV particles that can further infect B lymphocytes in vitro. We have shown that the SB-HCV strain could infect and replicate in T-cell lines and that HCV replication could inhibit interferon (IFN)-γ/signal transducer and activator of transcription-1 (STAT-1)/T-bet signaling of the T cells [13]. Moreover, we reported that HCV replication in Molt-4 could affect the proliferation and FAS-mediated apoptosis of T cells by inhibiting CD44v6 expression and mitogen-activated protein kinase (MAPK) signaling in Molt-4 [14]. Most of these data came from studies using cell lines, since stable SB-HCV replication could be detected in lymphoid cell lines (Raji, Molt-4, etc.). However, the analysis of primary lymphocytes is preferable to determine the real effects of lymphotropic HCV strains on T-cell biology. In fact, the effects of low titers of HCV in primary T cells have not been clarified yet.

We first reported that, among T cells, $CD4^+CD45RA^+RO^-$ naïve T cells were susceptible to SB-HCV infection [13]. Here we describe the functional and proliferative analysis of SB-HCV-infected naïve $CD4^+$ T cells after short-term culture.

## Materials and methods

### Culture of cell lines

SB cells that continuously produce infectious HCV particles were originally established from splenocytes of an HCV-infected patient with type 2 mixed cryoglobulinemia and monocytoid B-cell lymphoma [12]. The cells were maintained in standard RPMI (Invitrogen, Carlsbad, CA, USA) medium with 20% fetal bovine serum (FBS) without any supplement. Every 5 days, the cells were sedimented by natural gravity for 30 min at 37°C.

### In vitro infection of primary lymphoid cells

Supernatants from SB cells were purified by centrifugation and 0.2-μm filter. SB culture supernatant (5 ml), which contained $2.2 \times 10^4$ copies/ml of HCV RNA, was used for the infection of several kinds of human primary lymphoid cells ($1 \times 10^5$ cells). A control infection with UV-irradiated SB culture supernatant was included in every experiment. Supernatants of Huh7.5 cells transfected with JFH-1 strains [15–17] at 10 days post-transfection were used for several control experiments. Cells were washed 3 times at 2 days after infection. Then, a portion of the cells ($3 \times 10^5$ to $5 \times 10^5$ cells) was harvested for analysis; the remaining cells ($1 \times 10^5$ cells) were kept and incubated under the same condition.

### Isolation of various kinds of lymphoid cells and naïve $CD4^+$ T cells

We got informed consent from 5 healthy donors, from whom peripheral blood mononuclear cells (PBMC) were isolated by Ficoll-Paque centrifugation (Amersham Bioscience [Uppsala, Sweden]). Anti-CD3 phycoerythrin (PE), anti-CD4 (PE-Cy3), anti-CD8 (PE), anti-CD14 (PE), anti-CD19 (PE), anti-CD45RO (PE), and antiCD45RA (fluorescein isothiocyanate [FITC]) antibodies (BD Pharmingen) were used for the separation of different kinds of mononuclear cells by using fluorescence activated cell sorting (FACS) vantage (BD Parmingen, San Jose, CA, USA). In some experiments, a naïve $CD4^+$ T cell isolation kit II (Miltenyi Biotec [Bergish Gladbach, Germany]) was used to obtain more viable naïve $CD4^+$ cells.

### Strand-specific intracellular HCV RNA detection

Strand-specific intracellular HCV RNA was detected by using a recently established procedure that combined previously published methods [9, 18] with minor modifications [13]. Positive- and negative-strand-specific HCV RNAs were detected by a nested polymerase chain reaction (PCR) method. Reactions were performed with 2 μl of 10× reverse transcriptase (RT) buffer, 2 μl of 10-mmol/l magnesium chloride, 200-μmol/l each of deoxyadenosine triphosphate, deoxycytidine triphosphate, deoxyguanosine triphosphate, 100-μmol/l of thymidine triphosphate (dTTP), 0.2 U of uracil-*N* glycosylase (UNG; Perkin Elmer [Fremount, CA, USA]/Applied Biosystems), 5 U of rTth DNA Polymerase; and 50 pmol of strand-specific HCV primers (positions according to the 5′ untranslated region), nt −285 to −256 (ACTGTCTTCACGCAGAAAGCGTCT AGCCAT) and −43 to −14 (CGAGACCTCCCGGGGCA CTCGCAAGCACCC) and template RNA. The RT mixture was incubated for 10 min at room temperature and then at 70°C for an additional 15 min. The cDNA product was subjected to the first PCR with 80 μl of PCR reaction buffer containing 50 pmol of HCV downstream strand-specific primer. The PCR amplification consisted of 5 min at 95°C, followed by 35 cycles (1 min at 94°C, followed by 1 min at 67°C, and then by 1 min at 72°C), and then 7-min extension at 72°C. For the second nested PCR, an aliquot (1/10) of the first PCR reaction mixture was re-amplified

using 50 pmol of each of the two primers, nt −276 to −247 (ACGCAGAAAGCGTCTAGCCATGGCGTTAGT) and nt −21 to −50 (TCCCGGGGCACTCGCAAGCACCCT ATCAGG), which span the 255-base pair region nt −276 to −21 (position according to the 5′ untranslated region) of HCV RNA, and Taq polymerase (Applied Biosystems). The reaction was run for 35 cycles (1 min at 94°C, 1 min at 67°C, 1 min at 72°C), followed by 7 min at 72°C. Semi-quantification was achieved by serial fourfold dilutions (in 10 μg/ml of *Escherichia coli* tRNA) of an initial amount of 200 ng of total RNA. The relative titer was expressed as the highest dilution giving a visible band of the appropriate size on a 2% agarose gel stained by ethidium bromide. For internal control, semi-quantification of β-actin mRNA was performed by using the same RNA extracts. To rule out false, random, and self-priming, extracted HCV RNA was run in every RT–PCR test without the addition of an upstream HCV primer.

### CFSE staining

Cells were analyzed by using a CellTrace CFSE Cell Proliferation Kit (Invitrogen [Carlsbad, CA, USA]). The cell staining methods followed the manufacturer's protocol. Stained cells were washed three times and incubated for an additional 7 days. Cells were analyzed by flow cytometry with 510 nm excitation and emission filters. A proliferation index was calculated by FlowJo 7.5 (Tree Str Inc, Ashland, OR, USA), according to the manufacturer's protocol.

### Annexin V and propidium iodide staining

Cells were stained with Annexin V and propidium iodide (PI) by using an apoptosis detection kit (R&D systems, Minneapolis, MN, USA). Staining methods were conducted according to the manufacturer's protocol. Briefly, collected cells were washed and gently re-suspended in the Annexin V incubation reagent at a concentration of $3 \times 10^5$ cells per 100 μl. Then, re-suspended cells in binding buffer were stained by Streptavidin conjugate allophycocyanin (APC) and analyzed by flow cytometry within 1 h.

### Transfection of HCV individual protein expression plasmids

The various expression plasmids were constructed by inserting HCV core, E1, E2, NS3, NS4B, NS5A, and NS5B cDNA of genotype 1a [19] behind the cytomegalovirus virus immediate-early promoter in pCDNA3.1 (Invitrogen). Primary $CD4^+$ cells were transfected using Nucleofector I (Amaxa, Gaithersburg, Washington DC, USA) with a Human T cell Nucleofector kit (Amaxa), and various plasmids were purified using the EndFree plasmid kit (QIAGEN, Valencia, CA, USA). Viable transfected cells were isolated by Ficoll-Paque centrifugation (Amersham Bioscience) at 24 h post-transfection. Transfection and expression efficiency were analyzed by using intracellular staining of HCV individual proteins and flow cytometry analysis. Briefly, the cells were fixed and permeabilized with fixation/permeabilization solution (BD Bioscience) at 4°C for 25 min. The cells were then washed two times in BD Perm/Wash buffer (BD Bioscience) and resuspended in 50 μl of BD Perm/Wash buffer containing pre-conjugating polyclonal anti-E1, E2, NS3, NS4B, NS5B, NS5A antibody (abcam, Cambridge, MA, USA) with a phycoerythrin (PE)-conjugated anti-mouse antibody.

### Confocal laser microscopy

Primary lymphocytes ($3 \times 10^6$ cells/ml) in suspension were fixed and permeabilized with fixation/permeabilization solution (BD Bioscience) at 4°C for 25 min. The cells were then washed two times in BD Perm/Wash buffer (BD Bioscience) and resuspended in 50 μl of BD Perm/Wash buffer containing pre-conjugating polyclonal anti-NS5A antibody (Biodesign International, Saco, ME, USA) with an FITC-conjugated anti-mouse antibody.

### Interferon-γ and interleukin 10 secretion assay

Cells were washed by adding 2 ml of cold phosphate-buffered saline (PBS) and resuspended in 90 μl of cold RPMI 1640 medium. After the addition of 10 μl of IL-10- or IFN-γ-Catch Reagent (Miltenyi Biotec), cells were incubated for 5 min on ice. Then the cells were diluted with 1 ml of warm medium (37°C) and further incubated in a closed tube for 45 min at 37°C under slow continuous rotation. Cells were washed and IL-10- or IFN-γ-secreting cells were stained by adding 10 μL of IL-10- or IFN-γ-detection antibody (PE-conjugated) (Miltenyi Biotec) together with anti-CD4-PerCP.

### Real-time PCR analysis

Cells were collected sequentially at various time points after the addition of recombinant human IFN-γ (500 ng/ml) (BD Biosciences, CA, USA). After the extraction of total RNA and the RT procedure, real-time PCR using a TaqMan Chemistry System was carried out. The ready-made set of primers and probe for the amplification of T-bet (ID HS00203436) and glyceraldehyde-3-phosphate-dehydrogenase (GAPDH) were purchased from Perkin-Elmer/Applied Biosystems. The relative amount of target mRNA was obtained by using a comparative the threshold cycle (CT) method. The expression level of mRNAs of the non-stimulation sample of vector transfected-primary

$CD4^+$ cells was represented as 1.0 and the relative amount of target mRNA in a stimulated sample was calculated according to the manufacturer's protocol.

### Immunoblot assay

Proteins were resolved by electrophoresis in sodium dodecyl sulfate–polyacrylamide gels and electrophoretically transferred onto a polyvinylidene difluoride (PVDF) membrane (Bio-Rad, Hercules, CA, USA). The membrane was incubated with anti-STAT-1α, or anti-p-STAT-1 antibodies (Cell Signaling, Danver, MA, USA) and then reacted with peroxidase-conjugated secondary antibody. Immunoreactivity was visualized by an enhanced chemiluminescence detection system (Amersham Bioscience).

### Statistical analysis

Statistical analyses of the data in Figs. 1c, 2c, 3b, and 4 were performed by the analysis of variance (ANOVA)

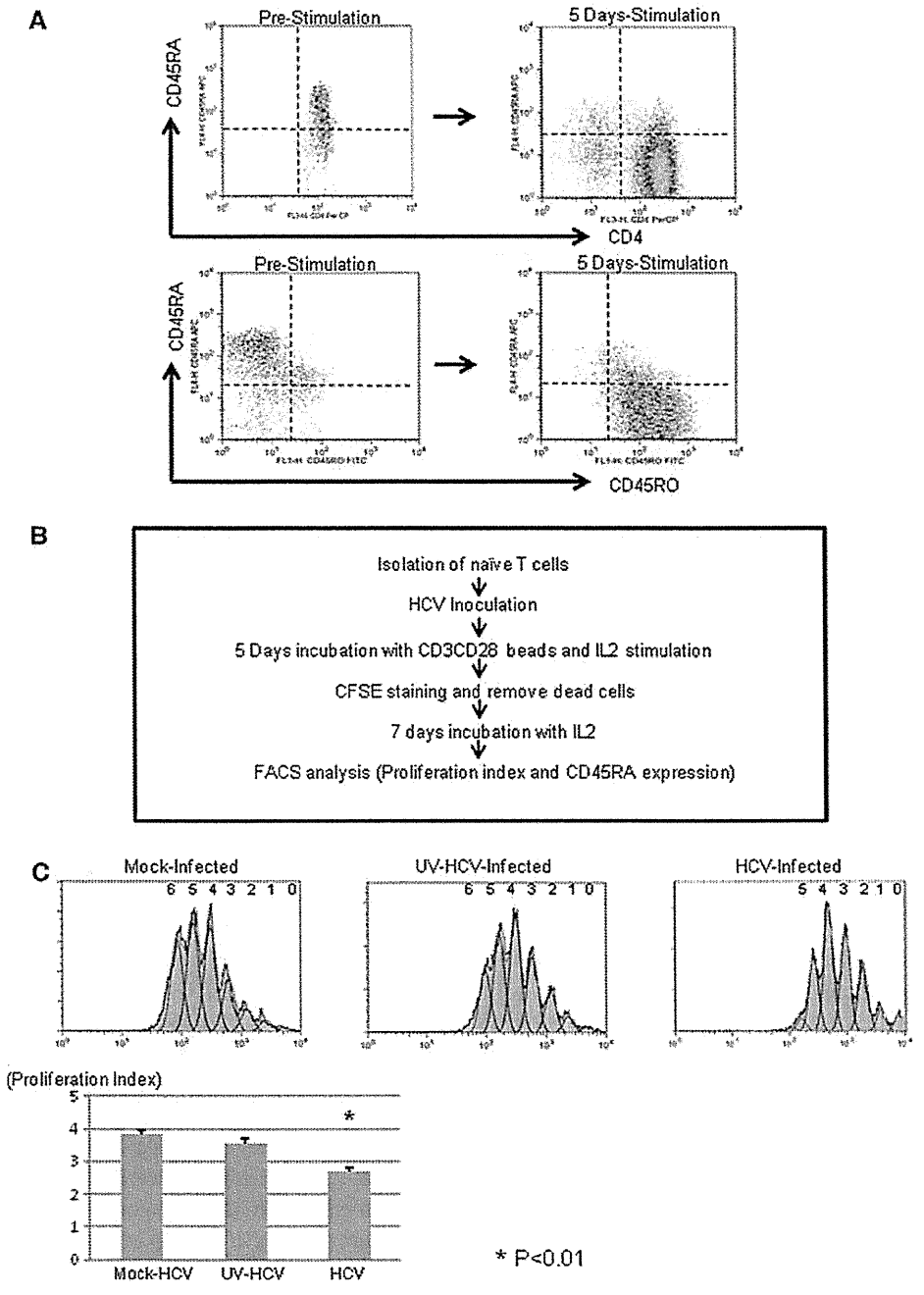


**Fig. 1** Suppression of proliferation activity in hepatitis C virus (*HCV*)-infected human naïve T lymphocytes. **a** A representative dot plot of $CD4^+CD45RA^+RO^-$ cells is shown. Cells are stained with CD4-PerCP-antibody (Ab), CD45RA-fluorescein isothiocyanate (FITC)-Ab, and CD45RO-APC-Ab. The purity of isolated $CD4^+CD45RA^+RO^-$ naïve T lymphocytes is over 92%. **b**, **c** Carboxyfluorescein succinimidyl ester (CFSE) staining was carried out at 5 days post-infection in SB-HCV, UV-irradiated HCV, and Mock. Stained cells were washed three times and incubated for an additional 7 days with T-cell expander. Cells were analyzed by flow cytometry with 510 nm excitation and emission filters. *Numbers* in the representative histogram indicate numbers of cell divisions. The proliferation index was calculated by FlowJo 7.5 software according to the manufacturer's protocol. The proliferation index is shown in this *bar graph*. Three independent experiments were carried out. *Error bars* indicate the standard deviation. *IL* interleukin

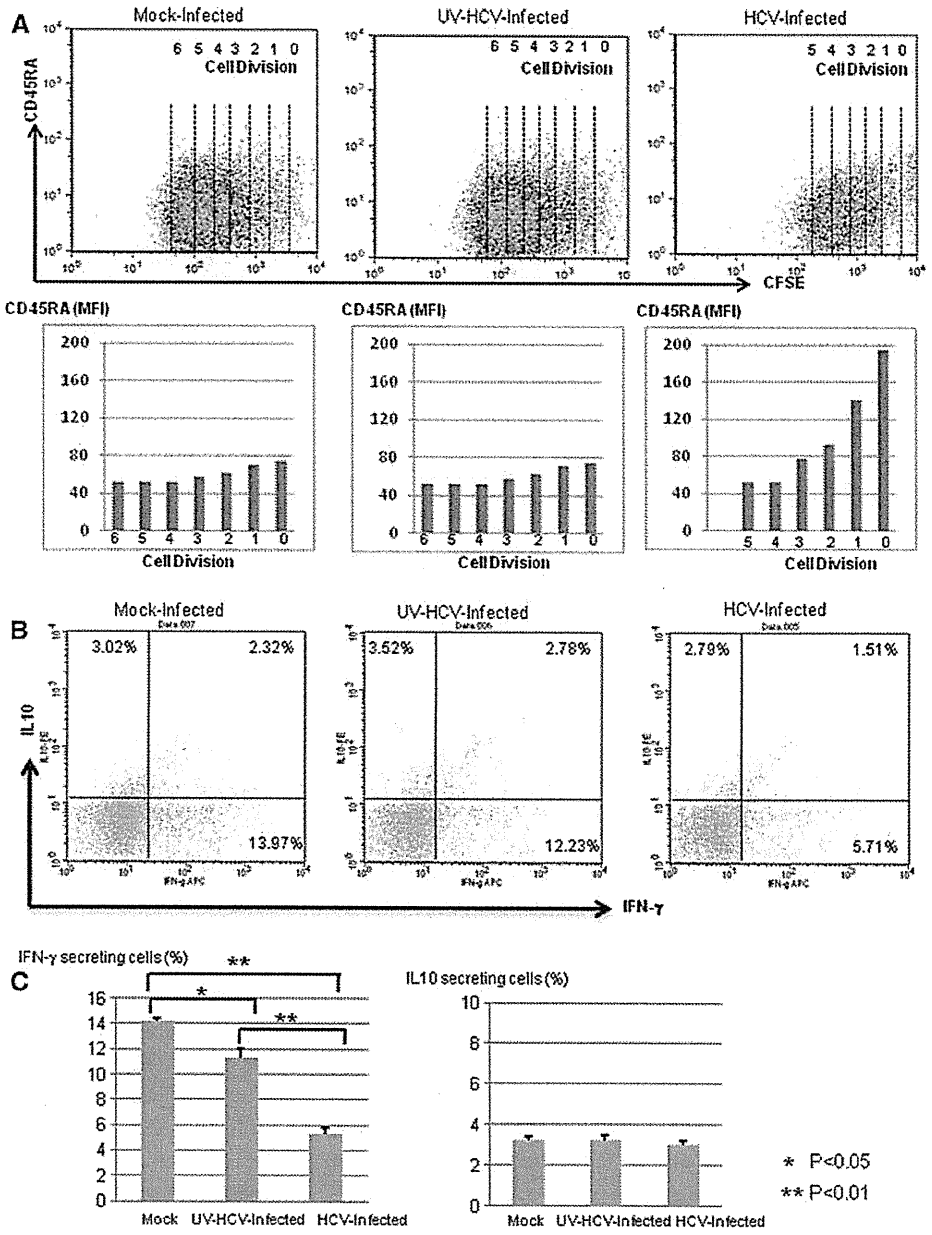


**Fig. 2** Suppression of development and Th1 commitment in HCV-infected human naïve T lymphocytes. **a** Representative dot plots of CD45RA and carboxyfluorescein succinimidyl ester (CFSE) double staining are shown. *Numbers* in the representative dot plots indicate the numbers of cell divisions. *Bar graphs* indicate the mean fluorescence intensity (MFI) of cell clusters. **b** Representative dot plots of interferon-γ (*IFN-γ*) and interleukin (IL) 10 secretion assays are shown. The *numbers* in the quadrant indicate IFN-γ and/or IL10-secreting cells among $CD4^+$ cells. **c** The frequencies of IFN-γ- and IL10-secreting cells among the three groups are shown in these *bar graphs*. Three independent experiments were carried out. *Error bars* indicate the standard deviation

test (SPSS10.0, SPSS Inc, Chicago, IL, USA). Values of $p < 0.05$ were considered to be statistically significant.

## Results

### Detection of negative-strand HCV-RNA among lymphoid cells

Strand-specific rTth based nested PCR was carried out to analyze the susceptibility to HCV infection among the various kinds of lymphoid cells with or without short term culture (7 days). Isolated lymphoid cells were infected with SB-HCV, UV-irradiated-HCV, or JFH-1 strain and were cultured with appropriate cytokines and/or antibody stimulation (Table 1). We needed to add different kinds of cytokines to maintain the cell proliferation and viability. Negative-strand HCV-RNA could be detected in $CD4^+$, $CD14^+$, and $CD19^+$ cells and in $CD8^+$ cell-depleted PBMCs ($PBMC\text{-}CD8^+$) after short-term culture (Table 2). However, negative- and positive-strand HCV-RNA could not be detected in any kinds of lymphoid cells infected with the supernatant of JFH-1 and JFH-1 GND mutant (data not shown). Undetectable negative-strand HCV-RNA at 2 days post-infection indicated that HCV-RNA was replicated after inoculation. We found that depletion of $CD8^+$ cells from

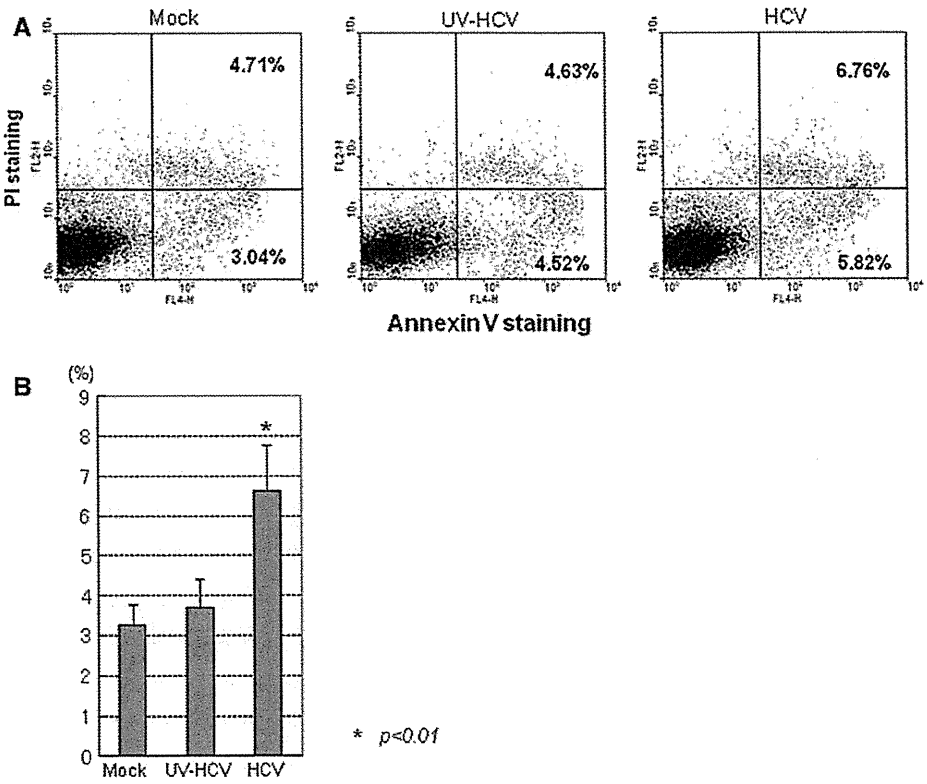


**Fig. 3** HCV replication induces apoptosis of naive $CD4^+$ cells. **a** Representative dot plots of Annexin V and propidium iodide (*PI*) staining are shown. The *numbers* in the quadrants indicate the frequencies of early apoptotic cells (Annexin $V^+$ and $PI^-$) and dead cells (Annexin $V^+$ and $PI^+$ cells). **b** The frequencies of early apoptotic cells are shown in this *bar graph*. Three independent experiments were carried out. *Error bars* indicate the standard deviations

PBMCs was favorable to replication in lymphoid cells. In this study, we used CD3CD28 beads and IL2 stimulation that could stimulate more efficiently than CD3 and IL2 stimulation. However, among the $CD4^+$ cells, $CD4^+$ $CD45RA^+RO^-$ naïve $CD4^+$ cells were most susceptible to infection, as we previously demonstrated (Table 2) (Suppl. Fig. 1) [13]. These data indicate that $CD4^+CD45RA^+RO^-$ naïve $CD4^+$ cells could be infected with SB-HCV during T-cell development. CD81 was one of the main candidates of HCV receptors for the infection of the cells [20–22]. We tried to analyze whether anti-CD81 antibody might block the SB-HCV infection of primarily naïve $CD4^+$ cells. HCV-NS5A protein could be detected in 12.2% of SB-HCV-inoculated naïve $CD4^+$ cells at 10 days post-infection. However, the pretreatment of anti-CD81 antibody reduced the frequency of NS5A detection among the SB-HCV-inoculated naïve $CD4^+$ cells (4.7%) (Suppl. Fig. 2). The sensitivity of NS5A immunostaining was lower than that of the strand-specific nested PCR method [13].

## Suppression of proliferation activity in SB-HCV-infected naïve $CD4^+$ cells

The purity of $CD45RA^+RO^-$ naïve $CD4^+$ cells after isolation was around 92% (Fig. 1a). CFSE staining was carried out at 5 days post-infection in SB-HCV, UV-irradiated HCV, and Mock. Stained cells were washed three times and incubated for an additional 7 days with T-cell expander (CD3CD28 coated beads and IL2 stimulation). Cells were analyzed by flow cytometry with 510 nm excitation and emission filters. The proliferation index was calculated by FlowJo 7.5 software according to the manufacturer's protocol. The proliferation index of SB-HCV-infected naïve $CD4^+$ cells was significantly lower than that of controls ($p < 0.01$) (Fig. 1b, c). These data indicate that lymphotropic SB-HCV suppresses the proliferation activity of T cells.

## Disturbance of cell development and IFN-γ-secreting activity

CD45RA and CFSE double staining was carried out to analyze the cell development. The expression level of CD45RA on naïve $CD4^+$ cells had gradually declined during cell proliferation. However, the CD45RA expression level of SB-HCV-infected naïve $CD4^+$ cells remained higher than those of the control groups (Fig. 2a). Moreover, the frequency of IFN-γ-secreting cells among SB-HCV-infected $CD4^+$ cells was significantly lower than those of the control groups ($p < 0.01$) (Fig. 2b, c). On the other hand, the frequency of IL10-secreting cells was comparable in the three groups (Fig. 2b, c). These data indicate that HCV infection could interrupt cell development, especially Th1 development.

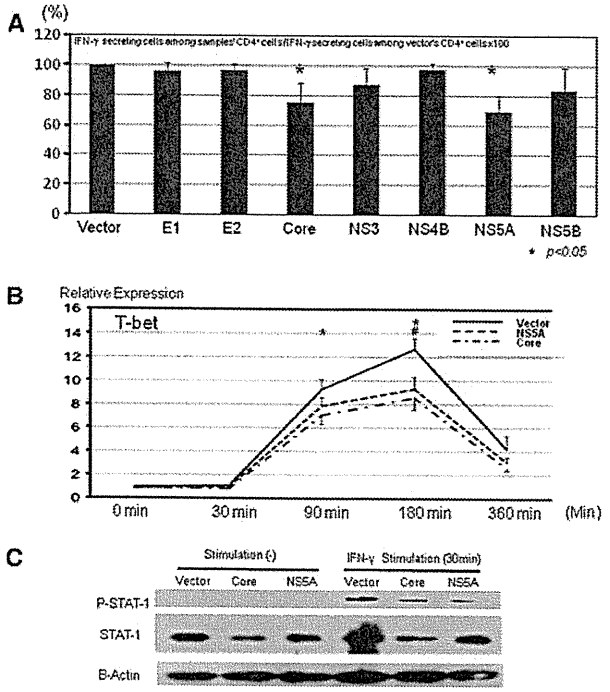


**Fig. 4** HCV-Core and NS5A proteins are the proteins that contribute to the suppression of IFN-$\gamma$ secretion. **a** HCV E1, E2, Core, NS3, NS4B, NS5A, and NS5B expression plasmids were used to transfect into primary $CD4^+$ lymphocytes by Nucleofector. The frequencies of IFN-$\gamma$-secreting cells among the samples' $CD4^+$ cells/the frequencies of IFN-$\gamma$-secreting cells among the vector's $CD4^+$ cells $\times 100$ are shown in this *bar graph*. **b** HCV core and NS5A transfected primary $CD4^+$ lymphocytes were stimulated with IFN-$\gamma$ (500 ng/ml). The relative expression of T-bet-mRNA was sequentially analyzed by real-time polymerase chain reaction (PCR). The relative amount of target mRNA was obtained by using a comparative the threshold cycle (CT) method. The expression level of mRNAs of the nonstimulation sample of vector transfected-primary $CD4^+$ cells is represented as 1.0 and the relative amount of target mRNA in a stimulated sample was calculated. Three independent experiments were carried out. *Error bars* indicate the standard deviation. **c** Immunoblotting assay was carried out to detect the protein of signal transducer and activator of transcription-1 (*STAT-1*), phospho-STAT-1 (*p-STAT-1*), and actin in the HCV-core, NS5A, and vector-plasmid transfected human primary $CD4^+$ cells with or without IFN-$\gamma$ stimulation (30 min)

## SB-HCV infection could induce apoptosis of naïve $CD4^+$ cells

Annexin V and PI double staining were carried out to detect early apoptotic cells. The frequency of Annexin-V-positive PI-negative early apoptotic cells in SB-HCV-infected naïve T cells was significantly higher than those in the control groups ($p < 0.01$) (Fig. 3a, b). UV-irradiated SB-HCV did not enhance the induction of apoptosis in naïve T cells with CD3CD28 stimulation. During T-cell activation, apoptosis is easily induced in order to maintain an appropriate immune response. In line with this feature, 3.04% of early apoptotic cells were detected in naïve T cells with CD3CD28 beads stimulation and Mock serum. These data indicate that SB-HCV replication could induce apoptosis, as seen in Molt-4 cells [14].

## HCV core and NS5A proteins could suppress IFN-$\gamma$ secretion from primary $CD4^+$ cells

We investigated the HCV proteins responsible for the suppression of IFN-$\gamma$ secretion. HCV E1, E2, Core, NS3, NS4B, NS5A, and NS5B expression plasmids were used to transfect into primary $CD4^+$ lymphocytes by Nucleofector. The intracellular staining of these proteins was carried out and the transfection efficiency was about 35–55% (Suppl. Fig. 3). Among these proteins, HCV core and NS5A could significantly suppress the IFN-$\gamma$ secretion ($p < 0.05$) (Fig. 4). HCV core and NS5A transfected primary $CD4^+$ lymphocytes were stimulated with IFN-$\gamma$. The relative expression of T-bet-mRNA was sequentially analyzed by real-time PCR. T-bet-mRNA expression in HCV core or NS5A transfected primary $CD4^+$ T lymphocytes was significantly suppressed at 90 and 180 min post-transfection in comparison to vector-transfected primary $CD4^+$ T lymphocytes. Moreover, the amount of STAT-1 protein in HCV-Core-expressing $CD4^+$ cells was remarkably lower than the amounts in vector and HCV-E2 transfected $CD4^+$ cells

**Table 1** Cytokine conditions for various kinds of lymphoid cell culture

| Cells | Cytokine condition | Other stimulant | Cell viability (%) |
|---|---|---|---|
| PBMC | IL2 (50 ng/ml) + IL6 (20 ng/ml) + CSF (250 ng/ml) | None | 80 |
| PBMC-CD8 | IL2 (50 ng/ml) + IL6 (20 ng/ml) + CSF (250 ng/ml) | None | 80 |
| CD3 | IL2 (50 ng/ml) | CD3CD28 coated beads | 70 |
| CD4 | IL2 (50 ng/ml) | CD3CD28 coated beads | 70 |
| CD8 | IL2 (50 ng/ml) | CD3CD28 coated beads | 70 |
| CD14 | CSF (250 ng/ml) | None | 60 |
| CD19 | IL-6 (20 ng/ml) | None | 70 |

The conditions of the cell culture are shown. Peripheral blood mononuclear cell (PBMC)-CD8 indicates CD8 cell-depleted PBMCs

*IL* interleukin, *CSF* colony stimulating factor

**Table 2** Strand-specific hepatitis C virus (HCV)-RNA detection in various kinds of lymphoid cells

| Subset | PBMC | PBMC-CD8 | CD3 | CD4 | CD8 | CD14 | CD19 |
|---|---|---|---|---|---|---|---|
| Positive strand | | | | | | | |
| 2 days | + | + | − | + | − | − | + |
| 7 days | ++ | ++ | + | ++ | − | ++ | +++ |
| 7 days UV-irradiated | − | − | − | − | − | − | − |
| Negative strand | | | | | | | |
| 2 days | − | − | − | − | − | − | − |
| 7 days | − | + | +/− | + | − | + | ++ |
| 7 days UV-irradiated | − | − | − | − | − | − | − |

| Subset | Whole $CD4^+$ | $CD4^+CD45RA^+RO^-$ | $CD4^+CD45RA^-RO^+$ |
|---|---|---|---|
| Positive strand | | | |
| 2 days | + | + | + |
| 7 days | ++ | +++ | + |
| 7 days UV-irradiated | − | − | − |
| Negative strand | | | |
| 2 days | − | − | − |
| 7 days | + | ++ | +/− |
| 7 days UV-irradiated | − | − | − |

Positive- and negative-strand-specific HCV-RNA was detected by semiquantitative nested polymerase chain reaction (PCR) methods

−, negative detection; +, positive detection without dilution; ++, positive detection with 4 times dilution; +++, positive detection with 16 times dilution; ±, only one detection in three independent experiments. Three independent experiments were carried out. Similar results were obtained three times

(Fig. 4c). The amount of phosphorylated STAT-1 (p-STAT-1) after IFN-γ stimulation was also analyzed. The amount of p-STAT-1 in HCV-Core and NS5A expressing $CD4^+$ cells was remarkably lower than that in the vector control.

## Discussion

There are many reports about the existence of extrahepatic HCV replication that might contribute to immune dysfunction [13, 14, 23–25]. We have reported that a specific SB-HCV strain could replicate in B- and T-cell lines and affect various immune systems [13, 14, 25]. However, the results of these studies were not definitely conclusive, since the cell lines were inappropriate to investigate the development and commitment of the lymphocytes. In the present study, we demonstrated that the SB-HCV strain could replicate in primary $CD19^+$ B cells, $CD4^+$ T cells, and $CD14^+$ monocytes with cytokine stimulation. Among the $CD4^+$ T cells, $CD4^+CD45RA^+RO^-$ naïve $CD4^+$ cells were the most susceptible to SB-HCV infection. One of the speculated reasons to explain why naïve $CD4^+$ cells with stimulation were most susceptible to SB-HCV infection is that T cells might temporarily express various kinds of molecules which may contribute to the HCV infection during T-cell development. The infectivity of naïve $CD4^+$ T cells was not as high as that of Molt-4 cells. However, significant suppression of cell development and IFN-γ secretion were seen in SB-HCV-infected naïve T cells with CD3, CD28, and IL2 stimulation. UV-irradiated-HCV that could not replicate in the cells suppressed the IFN-γ secretion slightly. These data indicate that not only the effect of HCV replication but also the direct binding effects of HCV structured proteins might contribute to the suppression of IFN-γ secretion. One report indicated that HCV-core protein could interact with the complement receptor gC1qR and upregulate suppressor of cytokine signaling-1 (SOCS-1), accompanied by downregulation of signal transducer and activator of transcription-1 (STAT-1) phosphorylation in T cells [7]. Another possible explanation of the discrepancies between HCV infectivity and suppression of proliferation and IFN-γ secretion might be the low sensitivity of HCV antigen-immunostaining, since lower sensitivity of immunostaining in comparison to the nested PCR method was found in our previous study [13].

HCV-Core and -NS5A proteins were the proteins responsible for the suppression of IFN-γ secretion from T cells. Lin et al. [26] have documented that HCV-core protein causes the degradation of STAT-1 protein and suppresses the Jak-STAT pathway in hepatocytes. In our previous study, reduction of STAT-1 protein was detected in HCV-core transfected primary naïve T cells and HCV-replicating Molt-4 cells [13]. Moreover, inhibition of intrahepatic gamma interferon production by HCV-NS5A

in transgenic mice was recently reported [27]. Recently, detection of HCV replicative intermediate RNA in perihepatic lymph nodes was reported [28]. The disturbance of Th1 commitment might influence the development of HCV-specific CTL in perihepatic lymph nodes. The selective infection of certain T cells by HCV in vivo may explain why there is only relative HCV-specific T-cell suppression without general immune suppression.

Suppression of proliferation activity was seen in HCV-infected naïve T cells as well as HCV-infected Molt-4 cells [14]. The expression level of CD45RA, which is a surface marker of T-cell development, gradually declined along with cell proliferation. However, HCV-infected naïve T cells expressed significantly higher levels of CD45RA than the control groups. We previously reported that HCV replication could suppress Ras/MEK/ERK signaling of Molt-4 [14]. During T-cell development, T cells showed strong proliferation activity that might facilitate HCV replication in T cells. However, extensive proliferation of HCV in T cells might interfere with the proper development of T cells.

The induction of apoptosis was seen in SB-HCV-infected naive T lymphocytes with CD3CD28 and IL2 stimulation. It is known that, during T-cell activation from naïve to effector cells, T cells have to survive activation-induced cell death (AICD), which may contribute to the maintenance of an appropriate level of the immune response [29, 30]. However, some groups reported that HCV replication could inhibit apoptosis in hepatoma cell lines [31, 32]. The developmental stages and characteristics of naïve T cells might explain these contradictory results. During T-cell activation, apoptosis is easily induced in order to maintain an appropriate immune response.

In conclusion, HCV replication in human naïve T cells might affect their proliferation activity and Th1 development, as was shown in the cell lines used in a previous study. The results suggest that the infectivity of HCV in human naïve T lymphocytes is low, although the biological effect of this infection might be significant because of its bystander effects.

**Acknowledgments** This work was supported in part by a Grant-in-Aid from the Ministry of Education, Culture, Sport, Science, and Technology of Japan (#21790642 to Y.K.), and by Health and Labour Sciences Research Grants for Research on Measures for Intractable Diseases (from the Ministry of Health, Labour and Welfare of Japan (to Y.U.). We are grateful to Dr. Michael M.C. Lai for providing the SB-HCV strain, and to Dr. Takaji Wakita for providing pJFH-1 and pJFH-1/GND.

## References

1. Alter MJ, Kruszon-Moran D, Nainan OV, McQuillan GM, Gao F, Moyer LA, et al. The prevalence of hepatitis C virus infection in the United States, 1988 through 1994. N Engl J Med. 1999; 341(8):556–62.
2. Chang KM, Rehermann B, Chisari FV. Immunopathology of hepatitis C. Springer Semin Immunopathol. 1997;19(1):57–68.
3. Ferri C, Caracciolo F, Zignego AL, La Civita L, Monti M, Longombardo G, et al. Hepatitis C virus infection in patients with non-Hodgkin's lymphoma. Br J Haematol. 1994;88(2):392–4.
4. Accapezzato D, Francavilla V, Paroli M, Casciaro M, Chircu LV, Cividini A, et al. Hepatic expansion of a virus-specific regulatory CD8(+) T cell population in chronic hepatitis C virus infection. J Clin Invest. 2004;113(7):963–72.
5. Manigold T, Racanelli V. T-cell regulation by CD4 regulatory T cells during hepatitis B and C virus infections: facts and controversies. Lancet Infect Dis. 2007;7(12):804–13.
6. Blackburn SD, Wherry EJ. IL-10, T cell exhaustion and viral persistence. Trends Microbiol. 2007;15(4):143–6.
7. Yao ZQ, Prayther D, Trabue C, Dong ZP, Moorman J. Differential regulation of SOCS-1 signalling in B and T lymphocytes by hepatitis C virus core protein. Immunology. 2008; 125(2):197–207.
8. Bare P, Massud I, Parodi C, Belmonte L, Garcia G, Nebel MC, et al. Continuous release of hepatitis C virus (HCV) by peripheral blood mononuclear cells and B-lymphoblastoid cell-line cultures derived from HCV-infected patients. J Gen Virol. 2005; 86(Pt 6):1717–27.
9. Hu Y, Shahidi A, Park S, Guilfoyle D, Hirshfield I. Detection of extrahepatic hepatitis C virus replication by a novel, highly sensitive, single-tube nested polymerase chain reaction. Am J Clin Pathol. 2003;119(1):95–100.
10. Laporte J, Bain C, Maurel P, Inchauspe G, Agut H, Cahour A. Differential distribution and internal translation efficiency of hepatitis C virus quasi species present in dendritic and liver cells. Blood. 2003;101(1):52–7.
11. Li Y, Wang X, Douglas SD, Metzger DS, Woody G, Zhang T, et al. CD8+ T cell depletion amplifies hepatitis C virus replication in peripheral blood mononuclear cells. J Infect Dis. 2005;192(6):1093–101.
12. Sung VM, Shimodaira S, Doughty AL, Picchio GR, Can H, Yen TS, et al. Establishment of B-cell lymphoma cell lines persistently infected with hepatitis C virus in vivo and in vitro: the apoptotic effects of virus infection. J Virol. 2003;77(3):2134–46.
13. Kondo Y, Sung VM, Machida K, Liu M, Lai MM. Hepatitis C virus infects T cells and affects interferon-gamma signaling in T cell lines. Virology. 2007;361(1):161–73.
14. Kondo Y, Machida K, Liu HM, Ueno Y, Kobayashi K, Wakita T, et al. Hepatitis C virus infection of T cells inhibits proliferation and enhances fas-mediated apoptosis by down-regulating the expression of CD44 splicing variant 6. J Infect Dis. 2009; 199(5):726–36.
15. Lindenbach BD, Evans MJ, Syder AJ, Wolk B, Tellinghuisen TL, Liu CC, et al. Complete replication of hepatitis C virus in cell culture. Science. 2005;309(5734):623–6.
16. Wakita T, Pietschmann T, Kato T, Date T, Miyamoto M, Zhao Z, et al. Production of infectious hepatitis C virus in tissue culture from a cloned viral genome. Nat Med. 2005;11(7):791–6.
17. Kato T, Date T, Murayama A, Morikawa K, Akazawa D, Wakita T. Cell culture and infection system for hepatitis C virus. Nat Protoc. 2006;1(5):2334–9.
18. Negro F, Krawczynski K, Quadri R, Rubbia-Brandt L, Mondelli M, Zarski JP, et al. Detection of genomic- and minus-strand of hepatitis C virus RNA in the liver of chronic hepatitis C patients by strand-specific semiquantitative reverse-transcriptase polymerase chain reaction. Hepatology. 1999;29(2):536–42.
19. Machida K, Cheng KT, Sung VM, Lee KJ, Levine AM, Lai MM. Hepatitis C virus infection activates the immunologic (type II) isoform of nitric oxide synthase and thereby enhances DNA

damage and mutations of cellular genes. J Virol. 2004;78(16): 8835–43.
20. Harris HJ, Farquhar MJ, Mee CJ, Davis C, Reynolds GM, Jennings A, et al. CD81 and claudin 1 coreceptor association: role in hepatitis C virus entry. J Virol. 2008;82(10):5007–20.
21. Molina S, Castet V, Pichard-Garcia L, Wychowski C, Meurs E, Pascussi JM, et al. Serum-derived hepatitis C virus infection of primary human hepatocytes is tetraspanin CD81 dependent. J Virol. 2008;82(1):569–74.
22. Cormier EG, Tsamis F, Kajumo F, Durso RJ, Gardner JP, Dragic T. CD81 is an entry coreceptor for hepatitis C virus. Proc Natl Acad Sci USA. 2004;101(19):7270–4.
23. Kanto T, Inoue M, Miyatake H, Sato A, Sakakibara M, Yakushijin T, et al. Reduced numbers and impaired ability of myeloid and plasmacytoid dendritic cells to polarize T helper cells in chronic hepatitis C virus infection. J Infect Dis. 2004; 190(11):1919–26.
24. Kanto T, Hayashi N, Takehara T, Tatsumi T, Kuzushita N, Ito A, et al. Impaired allostimulatory capacity of peripheral blood dendritic cells recovered from hepatitis C virus-infected individuals. J Immunol. 1999;162(9):5584–91.
25. Machida K, Kondo Y, Huang JY, Chen YC, Cheng KT, Keck Z, et al. Hepatitis C virus (HCV)-induced immunoglobulin hypermutation reduces the affinity and neutralizing activities of antibodies against HCV envelope protein. J Virol. 2008;82(13): 6711–20.
26. Lin W, Choe WH, Hiasa Y, Kamegaya Y, Blackard JT, Schmidt EV, et al. Hepatitis C virus expression suppresses interferon signaling by degrading STAT1. Gastroenterology. 2005;128(4): 1034–41.
27. Kanda T, Steele R, Ray R, Ray RB. Inhibition of intrahepatic gamma interferon production by hepatitis C virus nonstructural protein 5A in transgenic mice. J Virol. 2009;83(17):8463–9.
28. Pal S, Sullivan DG, Kim S, Lai KK, Kae J, Cotler SJ, et al. Productive replication of hepatitis C virus in perihepatic lymph nodes in vivo: implications of HCV lymphotropism. Gastroenterology. 2006;130(4):1107–16.
29. Krammer PH. CD95's deadly mission in the immune system. Nature. 2000;407(6805):789–95.
30. Holmstrom TH, Schmitz I, Soderstrom TS, Poukkula M, Johnson VL, Chow SC, et al. MAPK/ERK signaling in activated T cells inhibits CD95/Fas-mediated apoptosis downstream of DISC assembly. EMBO J. 2000;19(20):5418–28.
31. Nanda SK, Herion D, Liang TJ. The SH3 binding motif of HCV [corrected] NS5A protein interacts with Bin1 and is important for apoptosis and infectivity. Gastroenterology. 2006;130(3):794–809.
32. Miyasaka Y, Enomoto N, Kurosaki M, Sakamoto N, Kanazawa N, Kohashi T, et al. Hepatitis C virus nonstructural protein 5A inhibits tumor necrosis factor-alpha-mediated apoptosis in Huh7 cells. J Infect Dis. 2003;188(10):1537–44.

JOURNAL OF VIRAL HEPATITIS JVH

*Journal of Viral Hepatitis*, 2011, 18, 206–215 doi:10.1111/j.1365-2893.2010.01301.x

# Four-year study of lamivudine and adefovir combination therapy in lamivudine-resistant hepatitis B patients: influence of hepatitis B virus genotype and resistance mutation pattern

J. Inoue, Y. Ueno, Y. Wakui, H. Niitsuma, K. Fukushima, Y. Yamagiwa, M. Shiina, Y. Kondo, E. Kakazu, K. Tamai, N. Obara, T. Iwasaki and T. Shimosegawa *Division of Gastroenterology, Tohoku University Graduate School of Medicine, Aoba-ku, Sendai, Japan*

*Received September 2009; accepted for publication January 2010*

SUMMARY. To investigate the efficacy of long-term lamivudine (3TC) and adefovir dipivoxil (ADV) combination therapy in 3TC-resistant chronic hepatitis B virus (HBV) infected patients, we analysed 28 3TC-resistant patients treated with the combination therapy during 47 months (range, 9–75). At 12, 24, 36, and 48 months, the rates of virological response with undetectable HBV DNA (≤2.6 log copies/mL) were 56, 80, 86, and 92%, respectively. Among 17 hepatitis B e antigen (HBeAg)-positive patients, HBeAg disappeared in 24% at 12 months, 25% at 24 months, 62% at 36 months, and 88% at 48 months. When HBV genotypes were compared, patients with genotype B achieved virological response significantly more rapidly than those with genotype C ($P = 0.0496$). One patient developed virological breakthrough after 54 months, and sequence analysis of HBV obtained from the patient was performed. An rtA200V mutation was present in the majority of HBV clones, in addition to the 3TC-resistant mutations of rtL180M+M204V. The rtN236T ADV-resistant mutation was observed in only 25% clones. *In vitro* analysis showed that the rtA200V mutation recovered the impaired replication capacity of the clone with the rtL180M+M204V mutations and induced resistance to ADV. Moreover, rtT184S and rtS202C, which are known entecavir-resistant mutations, emerged in some rtL180M+M204V clones without rtA200V or rtN236T. In conclusion, 3TC+ADV combination therapy was effective for most 3TC-resistant patients, especially with genotype B HBV, but the risk of emergence of multiple drug-resistant strains with long-term therapy should be considered. The mutation rtA200V with rtL180M+M204V may be sufficient for failure of 3TC+ADV therapy.

*Keywords*: chronic hepatitis B, drug resistance, HBV, rtA200V.

## INTRODUCTION

Hepatitis B virus (HBV) causes acute and chronic infection, and chronic hepatitis often leads to liver cirrhosis and hepatocellular carcinoma (HCC) [1]. HBV contains a small (3.2 kb), circular, partially double-stranded DNA genome, and nucleoside or nucleotide analogues inhibit HBV replication by interfering with reverse transcriptase/DNA polymerase of the virus [2]. Although therapy with these drugs results in virological, biochemical, and histological improvement in most patients [3], the effect is often transient because of the emergence of drug-resistant HBV mutants [4].

Lamivudine (3TC), a nucleoside analogue of L-deoxycytidine, is associated with highly frequent emergence of drug-resistant mutants: the cumulative rate is about 20% per year [5,6]. Mutations that result in the replacement of methionine at amino acid 204 to valine or isoleucine (rtM204V/I) within the tyrosine-methionine-aspartate-aspartate (YMDD) motif in the reverse transcriptase (RT) region of HBV polymerase are found in most of the 3TC-resistant isolates [7]. Compensatory mutations rtV173L and rtL180M, which restore the replication capacity of the YMDD mutant *in vitro*, are observed frequently together with the YMDD mutation [8,9]. Adefovir dipivoxil (ADV) is a phosphonate nucleotide analogue of adenosine monophosphate, and ADV-resistance rates are lower than those of 3TC [10]. Two mutations, rtA181V/T and rtN236T, are associated with resistance to ADV [11–14], and the cumulative 5-year occurrence of genotypic resistance is reported to be 29% [15]. *In vitro* studies showed that these mutations confer a weaker

Abbreviations: ADV, adefovir dipivoxil; ALT, alanine aminotransferase; eGFR, estimated glomerular filtration rate; ETV, entecavir; HBeAg, hepatitis B e antigen; HBsAg, hepatitis B surface antigen; HBV, hepatitis B virus; HCC, hepatocellular carcinoma; PCR, polymerase chain reaction; RT, reverse transcriptase; TDF, tenofovir disoproxil fumarate.

Correspondence: Yoshiyuki Ueno, Division of Gastroenterology, Tohoku University Graduate School of Medicine, 1-1 Seiryo, Aoba-ku, Sendai 980-8574, Japan. E-mail: yueno@mail.tains.tohoku.ac.jp

decrease in the susceptibility to ADV, in comparison with the greater decrease in 3TC susceptibility because of the YMDD mutant [11,16]. This finding may explain the lower rate of the emergence of ADV resistance.

Although the number of approved drugs has increased in recent years, the treatment of chronic HBV infection remains a clinical challenge. Especially, how to manage drug-resistant patients including 3TC-resistant patients is a major problem. Continuation of 3TC monotherapy or retreatment with 3TC after its temporary discontinuation is ineffective options for 3TC-resistant patients [17]: the lack of any further benefit and the possibility of rapid re-emergence of resistant HBV have been reported [18]. Against 3TC-resistant HBV, ADV and entecavir (ETV) have a suppressive effect *in vivo* and *in vitro* [19–21]. Combination therapy of ADV and 3TC is effective for 3TC-refractory patients and has a low frequency of viral breakthrough [22]: the 3-year cumulative rate of *de novo* resistant mutants was 4% with no development of viral breakthrough in 3TC-resistant patients. However, further longer-term efficacy of the combination therapy remains unknown. ETV is a potent drug with infrequent development of resistance for treatment-naïve patients [23]. ETV monotherapy was shown to be effective during the first year of therapy in 3TC-resistant patients [20], but pre-existing 3TC-resistant mutants are favourable for the emergence of ETV resistance [21], and a comparatively high rate of the emergence of ETV-resistant strains has been reported in long-term studies [23]. Therefore, ETV monotherapy seems to be a less attractive option for the long-term treatment of 3TC-resistant patients.

Several previous reports have described the differences in the responses to antiviral therapy between HBV genotypes. A case–control study of 3TC treatment for genotypes B and C showed that the responses were not different, but the emergence of the YMDD mutation was more frequent in genotype C [24]. It was also reported that the YMDD mutation and breakthrough hepatitis developed more often in patients with genotype A than in patients with genotype B or C [25]. However, the impact of the genotype on the efficacy to ADV is uncertain.

Here, we studied the long-term efficacy of 28 3TC-resistant patients treated with the combination of 3TC and ADV and compared the response between HBV genotypes. Sequence analysis of HBV from a patient with resistance to the combination therapy was performed, and *in vitro* drug susceptibility of the mutant HBV clones was assessed to clarify the mechanism of the emergence of resistance.

## MATERIALS AND METHODS

### *Patients*

A total of 28 consecutive Japanese patients with chronic HBV infection who were treated with 3TC+ADV at Tohoku University Hospital from June 2003 to August 2009 for more than 6 months were enrolled in this study. All patients developed virological breakthrough during 3TC monotherapy, and ADV was added in. Virological breakthrough was defined as an increase in the serum HBV DNA level of ≥1 log copies/mL, which was determined using the Amplicor HBV monitor test (Roche Diagnostics, Tokyo, Japan), at two or more consecutive examinations in comparison with the lowest level after treatment. To evaluate renal function, the estimated glomerular filtration rate (eGFR) level using the Cockcroft-Gault formula [(140 - age) × (weight in kilograms) × (0.85 if female)/(72 × serum creatinine)] [26] was calculated. No patients were infected with HCV, nor had a history of other liver diseases. The patients were evaluated for the rate of virological response (undetectable HBV DNA: <2.6 log copies/mL), biochemical response [alanine aminotransferase (ALT) normalization: ≤35 IU/L], hepatitis B e antigen (HBeAg) loss, and virological breakthrough.

### *Antiviral treatment*

Adefovir dipivoxil was administered at a dosage of 10 mg/day in all but one patient in addition to 3TC at a dosage of 100 mg/day. One patient received 10 mg of ADV on alternate days and 50 mg/day of 3TC daily because of reduced eGFR at the start of treatment. This occurred when the eGFR level dropped to <50 mL/min.

### *Determination of HBV genotype*

The HBV genotype was determined as described previously [27] with minor modifications. Briefly, total DNA was extracted from 50 μL of serum sample by QIAamp Blood Mini kit (QIAGEN GmbH, Hilden, Germany) and subjected to nested polymerase chain reaction (PCR) with high fidelity polymerase (PrimeSTAR HS DNA polymerase; TaKaRa Bio Inc., Shiga, Japan), to amplify a 396-nt sequence in the S gene. The amplification products were sequenced on both strands directly using the BigDye Terminator v3.1 Cycle Sequencing kit on an ABI PRISM 3100 Genetic Analyzer (Applied Biosystems, Foster City, CA, USA). Sequence analysis was performed using Genetyx-Mac (Version 12.2.7; Genetyx Corp., Tokyo, Japan). The genotype of HBV was determined by phylogenetic analysis with HBV isolates whose genotype was known.

### *Sequencing analysis of HBV reverse transcriptase region*

Total DNA extracted from 50 μL of serum sample was subjected to nested PCR to amplify the 1148-nt sequence [nt 52 to 1199, the nucleotide numbers are in accordance with a genotype C HBV isolate of 3,215 nt (AB033550)] including the RT region of HBV polymerase. The first-round PCR was carried out with primers B026 [5′-TCA TCC WCA GGC CAT GCA GTG GA-3′ (W = A or T)] and B025 (5′-CTA GGA GTT CCG CAG TAT GGA TCG-3′), and the second round with

primers B011 [5′-YTT YCC TGC TGG TGG CTC CAG TTC-3′ (Y = C or T)] and B024 (5′-GGG GTT GCG TCA GCA AAC ACT TG-3′). The amplification products were sequenced on both strands directly or after cloning into pUC118. Sequencing analysis after cloning was performed at nt 497-1161.

### *Construction of plasmid*

A cloned mutant sequence including the RT region from a sample obtained after the development of 3TC and ADV resistance was digested with BlnI (TaKaRa Bio Inc.) and EcoT22I (TaKaRa Bio Inc.). The digested fragment (nt 179-1068) was ligated into the BlnI-EcoT22I site of pBFH2R, which contained a 1.3-fold HBV genome [28]. Quick Change II-E Site-Directed Mutagenesis kit (Stratagene, La Jolla, CA, USA) was used to introduce nucleotide substitutions into the plasmid. Each mutation found in the RT region, rtL180M [C to A at nt 667 (C667A)], rtT184S (A679T), rtA200V (C728T), rtS202C (A733T), rtM204V (A739G), and rtN236T (A836C), was converted into the wild type or another mutant nucleotide. To construct plasmids with combined nucleotide substitutions, these converted plasmids were used next as templates. As a result, variant constructs harbouring rtM204I, rtL180M+M204V, rtL180M+T184S+M204V, rtL180M+A200V+M204V, rtL180M+S202C+M204V, rtL180M+M204V+N236T, and rtL180M+A200V+M204V+N236T were composed, and all constructs were sequenced to confirm the nucleotide substitutions.

### *Cell culture and transfection*

Human hepatoma HepG2 cells were cultured in Dulbecco's modified Eagle medium supplemented with 10% bovine serum at 37 °C and 5% $CO_2$. Cells were seeded in 24-well plates at $1.25 \times 10^5$ cells/well. On the next day, 375 ng of plasmid DNA were transfected into these cells using TransIT LT-1 Transfection Reagent (Mirus, Madison, WI, USA), and cells were washed twice with phosphate-buffered saline after 4 h. Five hundred microliter of the medium and various amounts of adefovir (Toronto Research Chemicals Inc., Ontario, Canada) were added, and the culture supernatant was collected 4 days later. Experiments were performed at least in triplicate.

### *Real-time PCR and determination of $IC_{50}$*

HBV DNA in the culture supernatant was quantified by real-time PCR as described previously [28] to determine the 50% inhibitory concentration (IC50) for ADV of each mutant HBV clone. Briefly, to digest the input plasmid DNA in the culture supernatant, 5 μL of the supernatant were treated with 5 units of DNase I (TaKaRa Bio Inc.) at 37 °C for 2 h, and the reaction was stopped with EDTA. Then, total DNA was extracted with a QIAamp DNA Blood Mini kit, and 10 μL of 200 μL DNA solution were subjected to real-time PCR using a LightCycler (Roche Diagnostics). Dose–response curves were plotted to determine the ADV IC50.

### *Statistical analysis*

Statistical analyses were performed using Fisher's exact probability test for comparison of proportions between two groups and Mann–Whitney *U* test for comparison of continuous variables between two groups. The cumulative rate of undetectable HBV DNA or ALT normalization was calculated using the Kaplan–Meier method, and differences between the curves were tested using Log-rank test. Differences were considered to be statistically significant when $P < 0.05$.

## RESULTS

### *Study profile*

The demographic and clinical profiles of the 28 patients [20 men and 8 women, median age 53.5 years (range 18–72)] at commencement of 3TC+ADV therapy are shown in Table 1. One (3.6%), 7 (25.0%), and 19 (67.9%) patients had HBV of genotypes A, B, and C, respectively. Eight (28.6%) patients had cirrhosis, 7 (25.0%) had HCC, and 17 (60.7%) patients were HBeAg positive. The mutations of the YMDD motif were determined by direct sequencing, and the YIDD, YVDD, and YIDD+YVDD mixed pattern were found in 14 (50%), 11 (39%), and 2 (7%)of the patients, respectively. Only one (4%) patient had no mutation in the YMDD motif. There were no significant differences in the profiles between patients with genotype B and those with genotype C.

### *Response to lamivudine and adefovir dipivoxil combination therapy*

The 3TC-resistant patients treated with the combination therapy were followed up for a median of 47 months (range, 9–75). All patients continued to be treated with 3TC and ADV until virological breakthrough. The 6-, 12-, 24-, 36-, and 48-month rates of virological response with HBV DNA ≤ 2.6 log copies/mL were 39, 56, 80, 86, and 92%, respectively (Table 2). The ALT normalization rates were 57% at 6 months, 70% at 12 months, 84% at 24 months, 82% at 36 months, and 77% at 48 months. When compared between genotype B and C, the results of patients with genotype B tended to be favourable for both virological and biochemical response (Figs 1a,b). The cumulative probability of undetectable HBV DNA was significantly higher in genotype B than in genotype C ($P = 0.0496$), whereas there was no significant difference in that of ALT normalization. Notably, patients with genotype B achieved early virological response (HBV DNA < 2.6 log copies/mL at 6 months) significantly more frequently than those with genotype C

**Table 1** Demographic and clinical characteristics of the 28 lamivudine-resistant patients at the start of adefovir addition to the treatment

| | Overall ($n$ = 28)* | Genotype B ($n$ = 7) | Genotype C ($n$ = 20) |
|---|---|---|---|
| Age (years), median (range) | 53.5 (18–72) | 51.0 (18–72) | 53.5 (35–68) |
| Male patients, no. (%) | 20 (71.4) | 5 (71.4) | 14 (70.0) |
| Patients with cirrhosis, no. (%) | 8 (28.6) | 1 (14.3) | 7 (35.0) |
| Patients with HCC, no. (%) | 7 (25.0) | 0 (0) | 7 (35.0) |
| HBeAg positive, no. (%) | 17 (60.7) | 3 (42.9) | 13 (65.0) |
| HBV DNA (log copies/mL), median (range) | 7.6 (4.3 to >7.6) | 7.2 (5.3 to >7.6) | 7.6 (4.3 to >7.6) |
| Patients with rtM204 mutation (M:I:V:I/V, no.) | 1:14:11:2 | 1:3:2:1 | 0:11:8:1 |
| ALT (IU/L), median (range) | 86.5 (29–1027) | 314.0 (47–760) | 78.5 (29–1027) |
| T. Bil (mg/dL), median (range) | 1.1 (0.5–4.5) | 1.1 (0.5–1.5) | 1.1 (0.5–4.5) |
| Albumin (g/dL), median (range) | 4.1 (2.7–4.8) | 4.2 (3.8–4.8) | 4.0 (2.7–4.6) |
| Serum creatinine (mg/dL), median (range) | 0.7 (0.4–1.2) | 0.7 (0.6–1.2) | 0.7 (0.4–1.2) |
| Prior lamivudine therapy (month), median (range) | 28.6 (2–76) | 36.5 (2–76) | 28.6 (5–65) |

HCC, hepatocellular carcinoma; ALT, alanine aminotransferase; T. Bil, total bilirubin. *One patient had genotype A HBV.

**Table 2** Virological and biochemical response to lamivudine and adefovir combination therapy during a median of 47 months

| | Months of treatment | | | | | | |
|---|---|---|---|---|---|---|---|
| Response | 0 ($n$ = 28) | 6 ($n$ = 28) | 12 ($n$ = 27) | 24 ($n$ = 25) | 36 ($n$ = 22) | 48 ($n$ = 13) | 60 ($n$ = 7) |
| HBV DNA < 2.6 | 0 (0) | 11 (39.3) | 15 (55.6) | 20 (80.0) | 19 (86.4) | 12 (92.3) | 6 (85.7) |
| HBV DNA 2.6 to <5.0 | 1 (3.6) | 15 (53.6) | 11 (40.7) | 5 (20.0) | 3 (13.6) | 1 (7.7) | 1 (14.3) |
| HBV DNA ≥ 5.0 | 27 (96.4) | 2 (7.1) | 1 (3.7) | 0 (0) | 0 (0) | 0 (0) | 0 (0) |
| ALT normalization* | NA | 16 (57.1) | 19 (70.4) | 21 (84.0) | 18 (81.8) | 10 (76.9) | 6 (85.7) |
| HBeAg disappearance† | NA | 1/17 (5.9) | 4/17 (23.5) | 4/16 (25.0) | 8/13 (61.5) | 7/8 (87.5) | 4/5 (80.0) |
| Virological breakthrough | NA | 0 (0) | 0 (0) | 0 (0) | 0 (0) | 0 (0) | 1 (14.3) |

Values are shown as numbers of patients followed by percentages in parentheses. NA, not applicable. *ALT ≤ 35 IU/L. †Values are shown as numbers of patients/total followed by percentages in parentheses.

[5/7 (71%) vs. 5/20 (25%), $P$ = 0.0427]. Although the status of HBeAg at the start of ADV seemed to influence the response, the difference was not significant (Figs 1c,d). Among 17 HBeAg-positive patients, HBeAg disappeared in 6% at 6 months, 24% at 12 months, 25% at 24 months, 62% at 36 months, and 88% at 48 months. There was no patient with hepatitis B surface antigen (HBsAg) loss during follow-up in this study.

Three of 22 patients who were treated for more than 36 months did not achieve virological response. One of them developed virological breakthrough after 54 months of combination therapy. The other patients had 2.8 and 3.5 log copies/mL of serum HBV DNA at 36 months of therapy but did not develop breakthrough. None of the patients experienced biochemical breakthrough. One patient with HCC died of HCC progression at 9 months after ADV. None of the 21 patients without HCC at the start of ADV developed HCC during follow-up.

The renal toxicity with a ≥0.3 mg/dL increase in serum creatinine level was observed in five of the 28 patients. Two of them had a ≥0.5 mg/dL increase: the serum creatinine levels were increased from 0.8 to 1.4 mg/dL after 31 months in a patient, and from 0.9 to 1.7 mg/dL after 34 months in another patient. As their eGFR levels were lowered to 39 and 29 mL/min, the dosage of ADV was reduced to alternate-day administration. After the reduction of ADV, their serum creatinine and eGFR recovered.

### *Profile of a patient with lamivudine and adefovir dipivoxil resistance*

He was a 53-year-old Japanese man with HBeAg-positive liver cirrhosis at the start of 3TC monotherapy in April 2002. The genotype of HBV was found to be genotype C. His clinical course is shown in Fig. 2. He developed breakthrough hepatitis with serum HBV DNA of >7.6 log copies/mL and alanine aminotransferase (ALT) of 236 IU/L in March 2003. ADV was added to the ongoing 3TC therapy in June 2003, and HBV DNA was gradually reduced reaching <2.6 log copies/mL 3 years later. However, virological

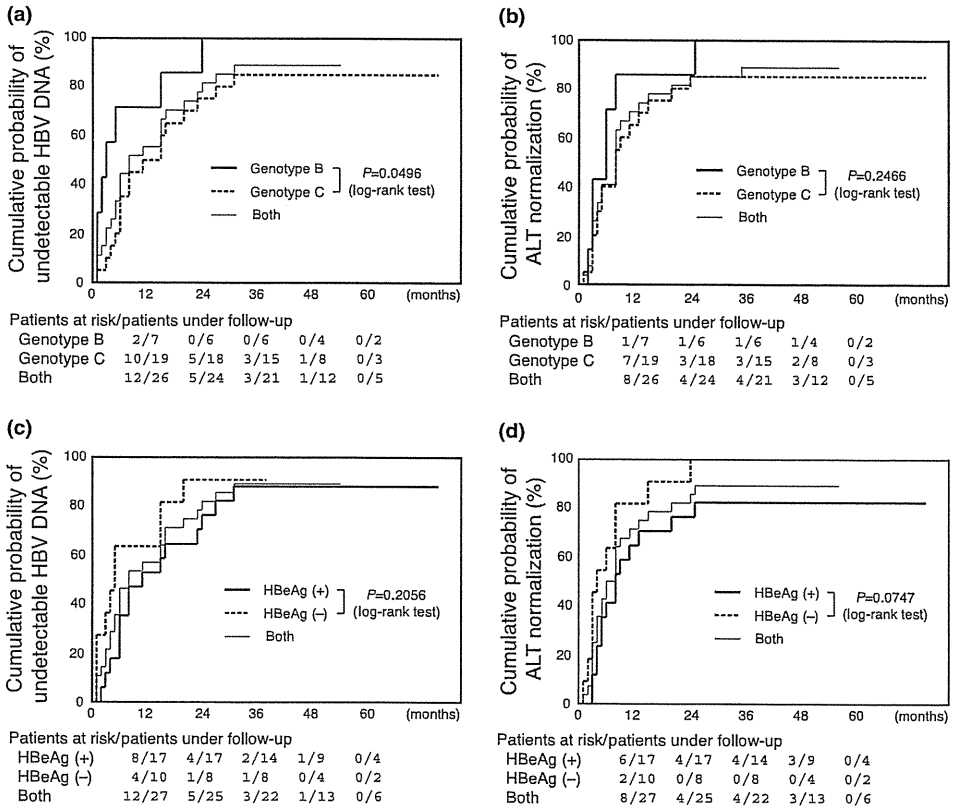


**Fig. 1** Cumulative probability of virological or biochemical response during lamivudine (3TC) and adefovir dipivoxil (ADV) combination therapy. (a) Cumulative probability of undetectable HBV DNA (<2.6 log copies/mL) in patients with genotype B and those with genotype C. (b) Cumulative probability of ALT normalization (≤35 IU/L) in patients with genotype B and those with genotype C. (c) Cumulative probability of undetectable HBV DNA in HBeAg-positive patients and HBeAg-negative patients. (d) Cumulative probability of ALT normalization in HBeAg-positive patients and HBeAg-negative patients.

breakthrough was observed at 4 years after starting ADV, and his HBV DNA reached 4.3 log copies/mL in December 2007. Because his liver was cirrhotic and the hepatic functional reserve was impaired, combination therapy of tenofovir disoproxil fumarate (TDF) and 3TC was started before ALT flair. Two months later, his HBV DNA was suppressed to <2.6 log copies/mL, and viral breakthrough has not been observed to date (20 months later).

### *Mutations found in the HBV reverse transcriptase region of the lamivudine and adefovir dipivoxil-resistant patient*

To investigate the mutations responsible for the viral breakthrough during the 3TC and ADV combination therapy, nucleotide sequences of the HBV RT region of the patient were compared between 3 time points: at the beginning of ADV treatment, at 30 months after ADV therapy, and at the time of viral breakthrough (54 months after ADV therapy). Direct sequencing analysis showed 10 amino acid changes during the clinical course (Fig. 2). The 3TC-resistant mutation of rtM204I changed to rtM204V after ADV treatment. Along with the change, the mixed mutation of rtL180L/M changed to rtL180M, which was reported to emerge with rtM204V during 3TC therapy [9]. The rtN236T mutation, which is a known ADV-resistance mutation [11], emerged as a mixed mutation with wild type (rtN236N/T) after viral breakthrough. Notably, rtA200V, which has never been reported as an ADV-resistant mutation, emerged also after viral breakthrough as a mixed mutation (rtA200V/A). Meanwhile, no specific mutation was found in the 2 patients without virological breakthrough who did not achieve virological response after 3 years of the combination therapy.

Clonal analysis was performed to examine the significance of these mutations of the RT region (Table S1). Several minor mutations were found during the 3TC and ADV therapy. After viral breakthrough, rtA200V was found in 63% of the clones, while rtN236T was found in only 25% of the clones. Therefore, rtA200V seemed to be responsible for the treatment failure of ADV. Moreover, rtT184S and S202C, which were reported as ETV resistance–associated mutations [29], were found as a minor population.

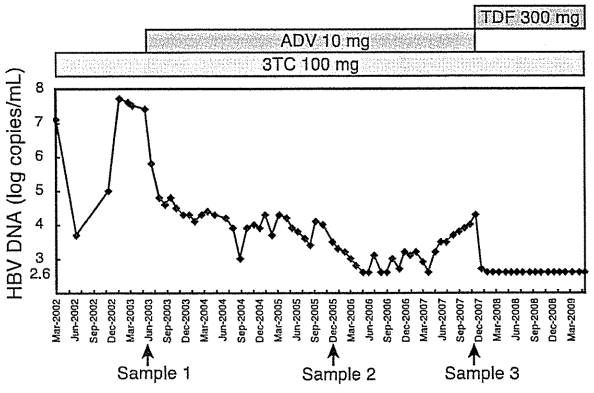


| RT mutation | L80 | P109 | D134 | R153 | L180 | A200 | M204 | V214 | L229 | N236 |
|---|---|---|---|---|---|---|---|---|---|---|
| Sample 1 | I/L | P/Q | G/D | R/Q | L/M | – | I | – | L/W | – |
| Sample 2 | – | – | – | – | M | – | V | A | – | – |
| Sample 3 | – | – | G/D | – | M | V/A | V | – | – | N/T |

**Fig. 2** Clinical course of a lamivudine (3TC)-resistant patient who developed virological breakthrough during 3TC and adefovir dipivoxil (ADV) combination therapy, and changes of amino acids in the reverse transcriptase (RT) region detected by direct sequencing analysis. After breakthrough, therapy was switched to 3TC plus tenofovir disoproxil fumarate (TDF) combination. The arrows indicate the time point when serum samples were obtained for sequencing analysis. Sample 1, 2, and 3 were obtained at the start of ADV, 30 months after ADV, and 54 months after ADV, respectively.

To investigate further the mutant populations, the combinations of these mutations and 3TC-resistant mutations were analysed (Fig. 3). At 30 months after ADV therapy, 100% of clones had mutations rtL180M+M204V. Subsequently, the mutations of rtT184S, A200V, S202C, and N236T emerged in the rtL180M+M204V clones after viral breakthrough. Of note, rtN236T was not found in clones without rtA200V.

### *Replication capacity and drug susceptibility of HBV mutants*

We analysed the replication capacity of HBV clones with combined mutations as shown in Fig. 3. A clone with rtL180M+M204V+N236T mutations, which was not found in the patient, was also included for comparison. Consistent with a previous report [30], 3TC-resistant mutations of rtM204I or rtL180M+M204V lowered the replication capacity significantly in comparison with the wild-type clone (Table 3). From additional mutations to rtL180M+M204V found in the patient, only rtA200V restored the impaired replication capacity significantly. The ETV-resistant mutation of rtT184S and rtS202C did not seem to have such an effect. The ADV-resistant mutation, rtN236T, lowered the replication capacity further, and rtA200V did not restore the lowered capacity caused by rtN236T.

The 7 HBV clones with mutations in the RT region were analysed for their susceptibility to ADV. The $IC_{50}$ of each clone is shown in Table 3. The clones with the 3TC-resistant mutations of rtM204I or rtL180M+M204V showed moderate resistance to ADV. In comparison with the clone with rtL180M+M204V, clones with additional mutations of rtT184S, A200V, or S202C showed significantly higher resistance to ADV. An additional mutation of rtN236T led to much greater resistance to ADV. Taking into account the results from the clonal analysis of serum samples and the replication capacity of each clone, rtA200V may be responsible for the treatment failure of 3TC+ADV therapy when it presents with 3TC-resistant mutations such as rtL180M+M204V. The mutations of rtT184S or S202C with rtL180M+M204V also confer ADV resistance, but the clones

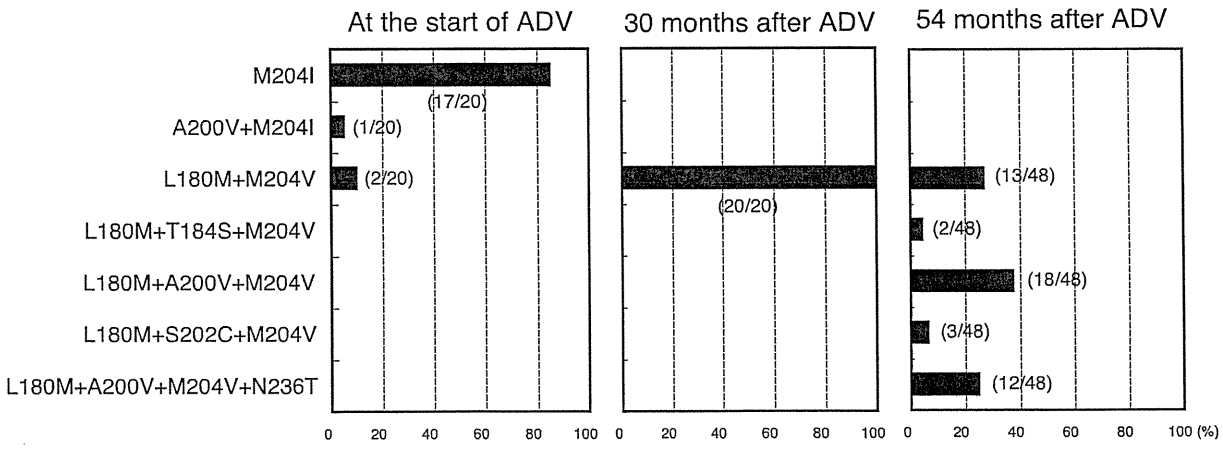


**Fig. 3** Clonal analysis of HBV obtained from the patient with 3TC and ADV resistance. The serum samples were collected at the time points indicated in Fig. 2. The percentages (no. of clones/total in parentheses) of the clones with the combined mutations in the RT region are shown.